

# PRELIMINARY CALCULATIONS ON ACTINIDE MANAGEMENT USING ADVANCED PWR MOX TECHNOLOGY

Author Jaakko Leppänen

Publicity public

<b>Research organisation and address</b> VTT Processes, P.O. Box 1604 FIN-02044 VTT, FINLAND	<b>Customer</b> Kauppa- ja Teollisuusministeriö, Valtion ydinjäterahasto	
<b>Project manager</b> Markku Anttila	<b>Contact person</b> Anne Väättäinen	
<b>Diary code (VTT)</b> PRO1-106T-03	<b>Order reference</b> 13/204/KYT	
<b>Project title and reference code</b> Suomalainen P&T-tekniikan tutkimus C2SU00084, 11TRANSMU	<b>Report identification &amp; pages</b> PRO1/P1007/05 40 p.	<b>Date</b> 22.3.2005

**Report title and author(s)**

Preliminary Calculations on Actinide Management Using Advanced PWR MOX Technology  
Jaakko Leppänen

**Summary**

The recycling of plutonium as MOX-fuel in light water reactors has been a part of the nuclear strategy in many European countries for several years. The currently applied mono-recycling can significantly reduce the production rate of new plutonium. The stabilisation of the buildup rate or the reduction of the existing stock, however, requires multi-recycling and advanced MOX technology. The research is under way and various advanced MOX fuel design concepts have been proposed and studied.

This report presents the preliminary results of a study, in which various reactor physical properties of a conventional PWR UOX and MOX assemblies are compared to the advanced MOX-UE concept. The MOX-UE assembly consists of a homogeneous lattice of MOX pins with multi-recycled plutonium and enriched-uranium support. Additional moderation is provided using extra water channels to compensate for the hardening of the flux spectrum due to the increased thermal absorption in the plutonium isotopes.

The calculations at this stage are focused on the safety-related features of the fuel. Various feedback coefficients, control worths and kinetic parameters are calculated using the MCNP4C Monte Carlo transport calculation code. To cope with the problem of higher actinide accumulation, assemblies with additional americium and curium are also studied. The future stages of the study will involve assembly-level burnup calculations using deterministic and Monte Carlo transport codes and finally full-core simulation with nodal diffusion codes.

**Distribution**
**Publicity**

public

**Project manager**
**Reviewed and approved by**

Markku Anttila

Antti Daavittila  
Group manager

Timo Vanttola  
Research manager

# Contents

<b>1</b>	<b>Introduction</b>	<b>3</b>
<b>2</b>	<b>Background</b>	<b>3</b>
2.1	Plutonium Management by Recycling . . . . .	3
2.2	Physical Features of MOX fuels . . . . .	4
2.3	Present Status of Plutonium Recycling . . . . .	5
2.4	Advanced MOX Design Concepts . . . . .	6
2.4.1	CORAIL . . . . .	6
2.4.2	APA . . . . .	6
2.4.3	MOX-UE . . . . .	7
<b>3</b>	<b>Geometry Model</b>	<b>7</b>
3.1	Geometry and Materials . . . . .	7
3.2	Isotopic compositions . . . . .	8
3.2.1	Fuel . . . . .	8
3.2.2	Burnable Absorbers . . . . .	11
3.2.3	Cladding . . . . .	13
3.2.4	Moderator . . . . .	13
3.2.5	Control Absorbers . . . . .	14
<b>4</b>	<b>Calculations</b>	<b>14</b>
4.1	Calculation Tools . . . . .	14
4.2	Calculation Cases . . . . .	14
4.2.1	Reference Cases . . . . .	14
4.2.2	MOX-UE Cases . . . . .	15
4.3	Calculated Parameters . . . . .	17
4.3.1	Fuel Temperature Coefficient . . . . .	17
4.3.2	Moderator Temperature Coefficients . . . . .	17
4.3.3	Soluble Absorber . . . . .	18
4.3.4	Control Rod Worths . . . . .	18



4.3.5	Delayed Neutron Fraction . . . . .	18
4.3.6	Prompt Neutron Lifetime . . . . .	19
4.3.7	Local Peaking Factor . . . . .	20
4.3.8	Performance Indicators . . . . .	20
4.3.9	Spectral Quantities . . . . .	21
<b>5</b>	<b>Results</b>	<b>21</b>
5.1	Production and Absorption Spectra . . . . .	21
5.2	Safety Parameters . . . . .	21
5.3	Fission Probabilities . . . . .	22
<b>6</b>	<b>Summary and Conclusions</b>	<b>22</b>

# 1 Introduction

Recycling plutonium in the commercial LWR fuel cycle has a promising potential for reducing the long-term radiotoxicity of disposed nuclear fuel. Presently, plutonium is recycled as mixed oxide (MOX) fuel in various countries, such as France and Belgium. The current mono-recycling strategies, however, do not take full advantage of the recycling potential and the buildup rate of plutonium can only be slowed down. Several advanced LWR MOX fuel concepts have been proposed in an effort to stabilise the plutonium buildup, or even to reduce the existing plutonium stock. The advanced fuel cycles involve multi-recycled plutonium and fully MOX loaded cores – two new features compared to the conventional MOX technology. In addition to plutonium, the recycling of higher actinides, americium and curium, in commercial light water reactors has also been studied.

This study compares various reactor physical properties of conventional PWR UOX and MOX fuels and advanced MOX fuels with multi-recycled plutonium and additional americium and curium. The reference cases are based on the preliminary design of the European Pressurised Reactor (EPR) fuel [1]. The advanced MOX assemblies are based on the homogeneous MOX-UE design concept [2] with additional moderation and enriched-uranium support.

This report presents the results of the first phase of the study. Steady-state calculations in a two-dimensional infinite-lattice geometry are performed using the MCNP4C Monte Carlo transport calculation code [3]. Various safety-related parameters, such as feedback coefficients, control worths and kinetic parameters are calculated. Fission-to-capture ratios of actinides are calculated as a first estimate of the transmutation efficiency of each fuel.

The next stage of the study will involve lattice-level burnup calculations using the deterministic lattice code CASMO and two Monte Carlo burnup calculation codes, Monteburns and MCB. Future studies will also include some cross section library comparison calculations. Finally, the third stage of this study will focus on core-level calculations using the SIMULATE and ARES nodal diffusion codes.

## 2 Background

### 2.1 Plutonium Management by Recycling

The isotopic composition of nuclear fuel changes as the fuel is burnt in the reactor. The composition tends to stabilise as the burnup increases, although the typical irradiation times are far too short for most isotopes to reach their equilibrium concentrations. If the initial concentration of some isotope is above the final equilibrium level, the isotope is

depleted during the irradiation. This is the main principle in plutonium management by recycling – excess plutonium from spent fuel is loaded into the core so that the transmutation rate exceeds the buildup rate of new material.

The transmutation efficiency depends on several factors, but the most significant variables are the total plutonium content and the level of neutron moderation. The range of practical plutonium loading is defined by various features related to reactor physics and nuclear safety. Present fuel fabrication technology and criticality safety restrictions limit the plutonium concentration of MOX fuel to about 12 wt-%.

The total fraction of fissile isotopes (Pu-239 and Pu-241) in the plutonium in disposed UOX fuel is slightly above 60 wt-%. After one recycle, this content has decreased to such low level (less than 50 wt-%) that the spent MOX fuel can not be used again without increasing either the plutonium content or the enrichment of the uranium support.

## 2.2 Physical Features of MOX fuels

The physical characteristics of mixed oxide fuels differ quite significantly from common uranium fuels. To some extent, a reactor loaded with MOX fuel resembles an UOX fuelled reactor at the end of the burnup cycle. The differences result from the relatively high concentration of plutonium isotopes. The primary fissile isotope is Pu-239 instead of U-235. The resonance region is more pronounced for plutonium isotopes and there are several low-energy peaks. MOX fuel pins are generally more absorbing at low energies, which results in a significant hardening of the flux spectrum.

These differences in the interaction physics lead to various reactor-physical differences between the fuel types:

1. Reactor time constants are different. The delayed neutron fraction of Pu-239 fission is only 0.0020 compared to the 0.0064 fraction in U-235 [4]. Increased neutron absorption shortens the mean neutron lifetime, i.e. the average time interval between the emission and the final absorption of a fission neutron. When these two factors are combined, the kinetic behaviour of the reactor becomes more problematic. The margin to prompt criticality is also decreased along with the effective delayed neutron fraction.
2. The high resonance peaks of plutonium isotopes, especially Pu-240, affect the reactivity feedback coefficients. The fuel Doppler and the moderator temperature coefficients tend to be more negative due to the increased absorption in the resonance region.
3. The role of thermal fission is less significant compared to UOX fuels, in which up to 80% of fissions are initiated by neutrons with energy less than 1 eV. For this reason,

the moderator void coefficient can be significantly less negative, or even positive if the plutonium content is too high. This is one of the main limiting factors in MOX fuel design.

4. The control worths of absorber rods and burnable and soluble absorbers are significantly lower compared to UOX fuels. This results from the fact that the absorber materials are most effective at low energies. The increased resonance absorption in the plutonium isotopes decreases the fraction of neutrons reaching thermal energies and eventually the fraction of neutrons absorbed in the control materials.

There are also other differences, not directly related to reactor operation. The higher accumulation rates of americium and curium isotopes, many of which are strong alpha emitters, lead to increased decay heat in irradiated MOX fuel. Spontaneous fission together with ( $\alpha$ , n) reactions increases the intrinsic neutron source. The handling and reprocessing of spent MOX fuel is technically more challenging compared to common UOX fuels.

### 2.3 Present Status of Plutonium Recycling

The commercial recycling of plutonium as conventional MOX fuel is established in various European countries, such as Belgium, France, Switzerland and Germany. There are also various reactors which are licenced to use MOX fuel and some in which MOX assemblies have been irradiated for experimental purposes. The history of commercial MOX recycling dates back to the early 1960's, when the first reprocessing and fabrication plants started operation in Belgium.

In France, plutonium recycling has been a part of the nuclear strategy since 1987 and in 2003, 22 reactors operated with partial MOX loading [5]. Mono-recycling in light water reactors, however, does not stabilise the overall plutonium inventory, although the buildup-rate can be significantly cut down. French legislation since 1991 requires that means to reduce the mass and toxicity of long-lived radionuclides is studied by nuclear proponents [6]. Plutonium and minor actinide recycling in light water reactors has had a significant role in this research and many of the studies referred to in this text have been carried out in French research organisations and industrial companies.

The currently applied recycling schemes involve mono-recycling and partially MOX-loaded cores ( $\sim 30\%$  MOX assemblies). The recycling is mainly done in PWRs. A typical PWR MOX assembly consists of several types of fuel rods with plutonium content varying from about 6 to 12 wt-%. The uranium oxide support is made of tail uranium with U-235 concentration of about 0.25 wt-%.

## 2.4 Advanced MOX Design Concepts

Advanced design concepts usually aim at zero or negative net production rate of plutonium, 100% MOX loading in the core, high burnup and multi-recycling of the spent fuel. The spectrum of innovative MOX design concepts is wide and there are several possibilities to increase the plutonium-burning capabilities. The penalties resulting from the increased plutonium content can be compensated by various design features. The following subsections introduce three near-term design concepts, which also summarise some of the leading ideas. More innovative designs can be found in reference [5]. Each of the three concepts are designed to be used with the current or near-future PWRs without major technical modifications.

### 2.4.1 CORAIL

The CORAIL concept<sup>1</sup> [7, 8, 9, 10] was proposed by CEA in 1999 as a medium term option for plutonium management. The assembly is a heterogeneous  $17 \times 17$  PWR lattice containing 180 standard UOX fuel rods and 84 MOX rods located in the periphery. The total plutonium content is kept down by restricting the Pu-concentration to about 8 wt-% in the MOX rods. To provide the excess reactivity and to level off the local peaking factor, the uranium enrichment of the UOX rods is raised to about 4.8 wt-%.

The assembly design is rather conservative and the fabrication does not require advanced technology, since both UOX and MOX rods are of the standard type. This simplicity is the main attractive feature in this design and makes it one of the most easily accessible options for plutonium multi-recycling. Fuel cycle studies [8] have shown that it is possible to attain zero net production rate of plutonium in an all-CORAIL nuclear park without compromising the required safety characteristics. Minor actinide recycling using CORAIL has also been studied [10] with some promising results.

### 2.4.2 APA

The advanced plutonium assembly (APA) concept [11] is more innovative compared to the CORAIL design. This design aims to improve the use of plutonium while minimising the production of minor actinides. The APA concept has been studied at CEA since 1995 and there are several variations to the basic design. The assembly is a  $17 \times 17$  PWR lattice in which the plutonium-bearing rods are locally over-moderated to compensate for the hardening of the flux spectrum. The additional moderation is realised by using either rods with reduced diameter or annular or cruciform rods which occupy the space of 4 standard rods. Both mixed oxide and inert matrix fuels have been studied as the material for the plutonium rods.

---

<sup>1</sup>Combustible Recyclable A Ilôt (recyclable fuel with islets)



Unlike with the CORAIL assembly, the manufacturing of the various APA designs requires technological development or at least major modifications to the present fuel fabrication facilities. The estimated performance of the APA fuel, however, is clearly better than that of the CORAIL. According to neutronic studies, it is possible to stabilise the plutonium inventory if 30% of the reactor park consists of full APA cores. In order to reach zero net production of both plutonium and minor actinides, 40% of the park is needed for the recycling.

### 2.4.3 MOX-UE

The development of the CORAIL and the APA concepts were suspended at CEA in 2002 and the research focused on the MOX-UE concept, which seems to be the option most compatible with the existing fuel cycle facilities [12]. The MOX-UE [2] is a homogeneous  $17 \times 17$  PWR assembly with 36 additional water rods to provide for extra moderation. The plutonium content of the first cycle MOX is about 9 wt-% and the uranium enrichment about 0.25 wt-%. When the plutonium quality degrades after successive recycles, both the plutonium content and the uranium enrichment are increased to gain more reactivity. Equilibrium in plutonium production is reached when 25-30% of the reactor park is fuelled with MOX-UE. The incineration of americium has also been studied and the stabilisation of both Pu and Am inventories seems feasible. The MOX-UE concept is taken as the basis for the advanced MOX fuel calculations in this study.

## 3 Geometry Model

### 3.1 Geometry and Materials

The geometry is an axially and radially infinite two-dimensional lattice of identical  $17 \times 17$  PWR fuel assemblies. The MCNP model covers a 1/8 of the assembly taking advantage of the symmetry of the pin layout. This study includes several types of UOX, conventional MOX and MOX-UE fuel assemblies. The details of each calculation case is described in section 4.2. The geometry is based on the preliminary EPR fuel assembly description given in reference [1]. The cross-sectional view of the reference UOX assembly is presented in Figure 1.

The essential geometry and material parameters are summarised in Table 1. Missing data are filled in using improvised values. It should be noted that the model used in these calculations is not a 100% accurate description of the EPR fuel lattice and especially the material data given in [1] contains several free parameters<sup>2</sup>. In order to avoid confusion in

---

<sup>2</sup>It should also be noted that the final design of the EPR fuel assembly is not yet fixed by the fuel manufacturer.

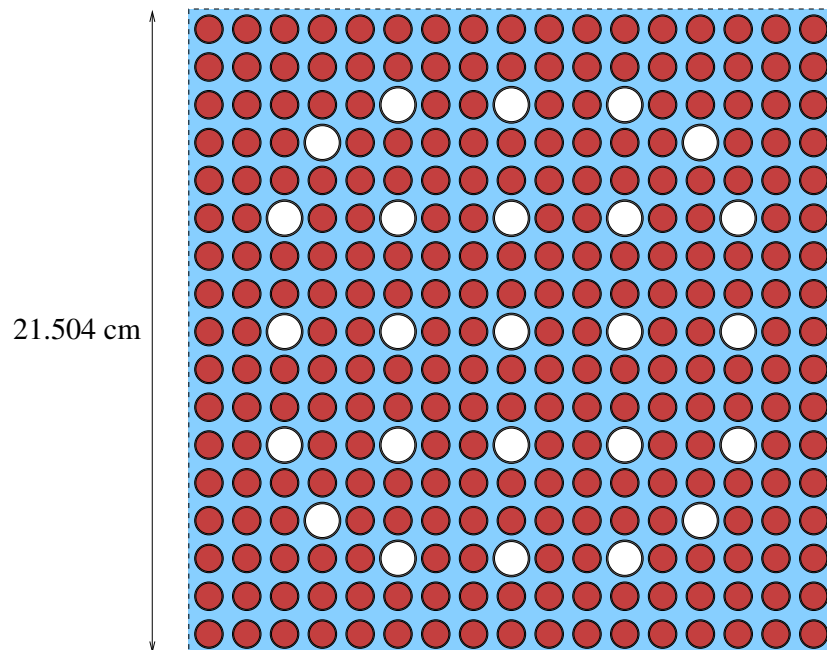


**Figure 1.** Cross-sectional view of the reference UOX fuel assembly. Fuel pins are red in colour and control rod thimble tubes white. The central tube is for instrumentation. When the control rods are not inserted, the tubes are filled with water.

the later stages, the material compositions used in the calculations are fixed and described in high detail in the following subsection.

## 3.2 Isotopic compositions

### 3.2.1 Fuel

Several fuel materials are used in the calculations. The basic assumption is that the material is in oxide form, i.e. the atomic ratio of heavy metal to oxygen is 1:2. For simplicity, it is always assumed that the total weight fraction of the heavy metal is 0.8815, or that the weight fraction of the fuel oxygen is

$$W_{O16} = 0.1185,$$

regardless of the detailed isotopic composition. The remaining part consists of uranium, plutonium and minor actinide isotopes.

The composition of the heavy metal is defined by the uranium enrichment  $\epsilon$ , the mass fractions of plutonium, americium and curium and their respective isotopic compositions.

**Table 1.** Essential geometry parameters for the 2D fuel assembly model [1].

	Parameter	Value
Assembly	Pin layout	17×17
	Number of fuel pins	264
	Number of control rod guide tubes	24
	Number of instrumentation tubes	1
Fuel pin	Assembly pitch	21.504 cm
	Fuel diameter	0.8725 cm
	Cladding inner diameter	0.8875 cm
	Cladding outer diameter	0.9500 cm
	Rod pitch	1.26 cm
	Fuel material	UO <sub>2</sub> (+ PuO <sub>2</sub> )
	Uranium enrichment	< 5.0 wt-%
	Total plutonium content	< 12.0 wt-%
	Fissile plutonium content	< 7.0 wt-%
	Fuel density*	10.5 g/cm <sup>3</sup>
	Cladding material	Zircaloy-2
	Cladding density	6.55 g/cm <sup>3</sup>
Guide thimble	Inner diameter**	1.1250 cm
	Outer diameter	1.2250 cm
	Material	Zircaloy-2
	Density	6.55 g/cm <sup>3</sup>
AIC absorber	Absorber diameter	0.765 cm
	Absorber density	10.17 g/cm <sup>3</sup>
	Canning inner diameter	0.772 cm
	Canning outer diameter	0.968 cm
	Canning material	stainless steel
B <sub>4</sub> C absorber	Canning density	7.9 g/cm <sup>3</sup>
	Absorber diameter	0.747 cm
	Absorber density	1.79 g/cm <sup>3</sup>
	Canning inner diameter	0.772 cm
	Canning outer diameter	0.968 cm
Coolant channel	Canning material	stainless steel
	Canning density	7.9 g/cm <sup>3</sup>
	Coolant temperature (core average)	310.15 °C
	Nominal coolant density***	0.70441 g/cm <sup>3</sup>

\* Fixed value, in reality depends on fuel composition.

\*\* Assuming thickness of 0.05 cm.

\*\*\* Corresponds to core average temperature and 15.5 MPa operating pressure.

The weight fractions of the uranium isotopes in the oxide are:

$$\begin{aligned}
 W_{U234}^U &= 0.8815 (1 - f_{Pu} - f_{Am} - f_{Cm}) w_{U234}^U \\
 W_{U235}^U &= 0.8815 (1 - f_{Pu} - f_{Am} - f_{Cm}) \epsilon \\
 W_{U238}^U &= 0.8815 (1 - f_{Pu} - f_{Am} - f_{Cm}) (1 - w_{U234}^U - \epsilon)
 \end{aligned} \tag{1}$$

where  $f_{Pu}$ ,  $f_{Am}$  and  $f_{Cm}$  are the total mass fractions of the plutonium, americium and curium isotopes, respectively. Fraction  $w_{U234}^U$  defines the content of U-234 in uranium and is related to the U-235 enrichment by:

$$w_{U234}^U = 0.008 \epsilon .$$

The plutonium vector defines the relative mass fractions of the isotopes. Recycled reactor-grade plutonium typically contains also trace amounts of Am-241. The compositions of additional americium and curium are defined in a similar manner. The isotopic mass fractions of the three elements in the oxide fuel are given by:

$$\begin{aligned}
 W_i^{Pu} &= 0.8815 f_{Pu} w_i^{Pu} \\
 W_i^{Am} &= 0.8815 f_{Am} w_i^{Am} \\
 W_i^{Cm} &= 0.8815 f_{Cm} w_i^{Cm}
 \end{aligned} \tag{2}$$

where  $w_i^{Pu}$ ,  $w_i^{Am}$  and  $w_i^{Cm}$  are the isotopic coefficients in the Pu, Am and Cm vectors. It should be noted that the total mass fraction of Am-241 in the fuel is

$$W_{Am241}^{tot} = W_{Am241}^{Pu} + W_{Am241}^{Am} ,$$

if excess americium is added in a MOX fuel already containing some Am-241.

The plutonium vectors for the MOX fuels used in this study are given in Table 2. The reference MOX corresponds to the composition given in the EPR fuel description [1]. MOX-A, MOX-B and MOX-C refer to different compositions used in the MOX-UE calculations. MOX-A is first cycle MOX and represents the plutonium composition of disposed UOX fuel. This composition is very close to the reference EPR MOX. MOX-B is equilibrium MOX and refers to a composition that has been stabilised after a large number of recycles. MOX-C is a combination of first and second cycle MOX. The latter three compositions are taken from reference [2].

The isotopic compositions of americium and curium in spent fuel depend significantly on the fuel type, the discharge burnup and the overall cooling time. The additional americium in these calculations consists of 75 wt-% Am-241 and 25 wt-% Am-243. This composition is a compromise between americium in spent UOX and MOX fuels [2]. The additional curium is assumed to be extracted from discharged MOX fuel after 7 years of cooling. The isotopic fractions are: 1 wt-% Cm-243, 84 wt-% Cm-244 and 15 wt-% Cm-245 [13].

**Table 2.** Plutonium vectors of the reference EPR MOX [1] and MOX-UE fuels [2].

Isotope	reference MOX	MOX-A	MOX-B	MOX-C
Pu-238	4.0 wt-%	2.7 wt-%	4.3 wt-%	4.0 wt-%
Pu-239	50.0 wt-%	56.0 wt-%	36.6 wt-%	43.9 wt-%
Pu-240	23.0 wt-%	25.9 wt-%	26.8 wt-%	28.7 wt-%
Pu-241	12.0 wt-%	7.4 wt-%	11.0 wt-%	11.7 wt-%
Pu-242	9.5 wt-%	7.3 wt-%	20.2 wt-%	10.5 wt-%
Am-241	1.5 wt-%	0.7 wt-%	1.1 wt-%	1.2 wt-%
fissile (239 + 241)	62.0 wt-%	63.4 wt-%	47.6 wt-%	55.6 wt-%

### 3.2.2 Burnable Absorbers

Natural gadolinium and erbium are used as burnable absorbers in oxide form. The description of the EPR fuel assembly [1] includes only gadolinium as a burnable absorber. The use of erbium was included in this study for the sake of completeness. The absorber material is homogeneously mixed with the oxide fuel. The isotopic composition is determined by the absorber content,  $f_{ba}$ , i.e. the mass fraction of  $Gd_2O_3$  or  $Er_2O_3$  in the fuel. The mass fractions of the heavy metal isotopes in doped fuel pins are given by Equations (1) and (2), multiplied by  $(1 - f_{ba})$ .

The isotopic compositions of natural Gd and Er are given in Table 3. The total gadolinium and oxygen mass fractions in  $Gd_2O_3$  are 0.8676 and 0.1324 and the mass fractions of erbium and oxygen in  $Er_2O_3$  0.8745 and 0.1255. The mass fraction of gadolinium isotope  $i$  in the doped fuel is hence given by

$$W_i^{Gd} = 0.8676 f_{ba} w_i^{Gd},$$

if the burnable absorber is  $Gd_2O_3$  and the mass fraction of erbium isotope  $i$  by

$$W_i^{Er} = 0.8745 f_{ba} w_i^{Er},$$

if the absorber is  $Er_2O_3$ . The coefficients  $w_i^{Gd}$  and  $w_i^{Er}$  are the mass fractions of the isotopes in natural Gd or Er, respectively. The mass fraction of oxygen in fuel doped with burnable absorber is then

$$W_{O16} = 0.1324 f_{ba} + 0.1185 (1 - f_{ba})$$

in the case of  $Gd_2O_3$  and

$$W_{O16} = 0.1255 f_{ba} + 0.1185 (1 - f_{ba})$$

in the case of  $Er_2O_3$ , respectively.

**Table 3.** *Isotopic compositions of the elemental materials.*

element	Isotope	Atom fraction	Mass fraction
Gadolinium	Gd-152	2.00000E-03	1.93218E-03
	Gd-154	2.10000E-02	2.05551E-02
	Gd-155	1.48000E-01	1.45808E-01
	Gd-156	2.06000E-01	2.04259E-01
	Gd-157	1.57000E-01	1.56673E-01
	Gd-158	2.48000E-01	2.49061E-01
	Gd-160	2.18000E-01	2.21711E-01
Erbium	Er-162	1.40000E-03	1.35535E-03
	Er-164	1.56000E-02	1.52890E-02
	Er-166	3.34000E-01	3.31340E-01
	Er-167	2.29000E-01	2.28548E-01
	Er-168	2.71000E-01	2.72085E-01
	Er-170	1.49000E-01	1.51382E-01
Boron	B-10	2.00000E-01	1.85272E-01
	B-11	8.00000E-01	8.14728E-01
Silver	Ag-107	5.18300E-01	5.13673E-01
	Ag-109	4.81700E-01	4.86327E-01
Indium	In-113	4.30000E-02	4.22835E-02
	In-115	9.57000E-01	9.57716E-01
Cadmium	Cd-106	1.30000E-02	1.22484E-02
	Cd-108	8.90000E-03	8.54349E-03
	Cd-110	1.25000E-01	1.22215E-01
	Cd-111	1.28000E-01	1.26288E-01
	Cd-112	2.41100E-01	2.40016E-01
	Cd-113	1.22000E-01	1.22538E-01
	Cd-114	2.87000E-01	2.90818E-01
Cd-116	7.50000E-02	7.73336E-02	

Unfortunately, the ENDF/B-VI.8 evaluated data file used in these calculations only contains cross section data for erbium isotopes Er-166 and Er-167<sup>3</sup>. For this reason, the isotopic composition of natural erbium had to be modified from the composition given in Table 3. The capture cross section of natural Er is entirely dominated by the odd-N isotope Er-167. The remaining even-N isotopes not included in the cross section data were therefore simply added to the fraction of Er-166. This simplification is well justified for steady state calculations. In burnup calculation, however, errors may arise in the depletion of the erbium isotopes.

<sup>3</sup>All isotopes in natural erbium are included in the more recently published JEFF-3.0 and JENDL-3.3 data files.

### 3.2.3 Cladding

The cladding and thimble tube material is Zircaloy-2 and it remains the same in all calculations. The canning material of the control rods is stainless steel. The material compositions are given in Table 4. Since cross section libraries exist for the elemental materials, there is no need to divide the components into separate isotopes. The atom fractions are also given in Table 4 for the sake of completeness.

**Table 4.** Material compositions of the cladding materials.

Material	Isotope	Atom fraction	Mass fraction
Zircaloy-2	Zr-nat	9.77015E-01	9.81350E-01
	Sn-nat	1.10948E-02	1.45000E-02
	Fe-nat	2.19542E-03	1.35000E-03
	O-16	7.09731E-03	1.25000E-03
	Cr-nat	1.74662E-03	1.00000E-03
	Ni-nat	8.51115E-04	5.50000E-04
Stainless steel	Fe-nat	6.75500E-01	6.84000E-01
	Cr-nat	1.84558E-01	1.74000E-01
	Ni-nat	1.09950E-01	1.17000E-01
	Mn-55	1.99770E-02	1.99000E-02
	Si-nat	1.00148E-02	5.10000E-03

### 3.2.4 Moderator

The moderator contains four isotopes: H-1, O-16, B-10 and B-11. The mass fractions of these isotopes are calculated from:

$$W_{\text{H1}} = 0.1146(1 - C_b)$$

$$W_{\text{O16}} = 0.8854(1 - C_b)$$

$$W_{\text{B10}} = C_b w_{\text{B10}}$$

$$W_{\text{B11}} = C_b(1 - w_{\text{B10}})$$

where  $C_b$  is the boron mass fraction in water and  $w_{\text{B10}}$  is the enrichment of boron with respect to B-10 ( $w_{\text{B10}} = 0.1853$  for natural boron, see Table 3). It should be noted that in reality boron is dissolved in the water as boric acid ( $\text{HBO}_3$ ), not as elemental boron. In reactor physics calculations, however, the boron concentration is often given directly as the elemental mass fraction of natural or enriched boron in units of ppm. The hydrogen and oxygen in boric acid are insignificant and not included in the composition at all.

### 3.2.5 Control Absorbers

Two types of absorber materials are used in control rods: boron carbide ( $B_4C$ ) and AIC. The mass fractions of boron and carbon in  $B_4C$  are 0.7826 and 0.2174, respectively. The AIC absorber consists of 80.0 wt-% silver, 15.0 wt-% indium and 5.0 wt-% cadmium. The detailed isotopic compositions can be calculated from these elemental mass fractions by multiplying with the corresponding isotopic mass fractions in Table 3.

## 4 Calculations

### 4.1 Calculation Tools

The calculations at this stage of the study were carried out using the MCNP4C Monte Carlo transport calculation code [3] and ENDF/B-VI.8 based multi-temperature cross section data libraries with delayed neutron data, generated at the Royal Institute of Technology, Sweden. A total of 50 million neutron histories were simulated in each case (1000 active cycles of 50000 neutrons). The running time on a 12 processor 2.4 GHz AMD Opteron cluster ranges from about 40 to 100 minutes, depending on the calculation case. The statistical error of  $k_{\text{eff}}$  in the criticality calculations was very low, in the order of 0.00010.

### 4.2 Calculation Cases

The calculation cases are divided into reference cases involving conventional UOX and MOX lattices and burnable absorbers and MOX-UE cases, which are based on the innovative design. Some of the MOX-UE cases also deal with the incineration of additional americium and curium. The boron concentration of the moderator was zero in all cases.

#### 4.2.1 Reference Cases

Six cases based on the reference EPR fuel description [1] were included in the study. The results of these cases will be used as reference values and compared to the results of the advanced MOX-UE calculations. The reference cases are:

**Case 1:** Reference EPR UOX lattice. Uranium enrichment 4.7 wt-% with respect to U-235. No plutonium or minor actinide isotopes in the fuel.

**Case 2:** Reference EPR UOX lattice + 8 burnable absorber pins containing 8 wt-% natural gadolinium. Uranium enrichment 4.7 wt-% in normal fuel pins and 0.25 wt-% in Gd pins.



- Case 3:** Reference EPR UOX lattice + 20 burnable absorber pins containing 8 wt-% natural gadolinium. Uranium enrichment 4.7 wt-% in normal fuel pins and 0.25 wt-% in Gd pins.
- Case 4:** Reference EPR UOX lattice + 8 burnable absorber pins containing 8 wt-% natural erbium. Uranium enrichment 4.7 wt-% in normal fuel pins and 0.25 wt-% in Er pins.
- Case 5:** Reference EPR UOX lattice + 20 burnable absorber pins containing 8 wt-% natural erbium. Uranium enrichment 4.7 wt-% in normal fuel pins and 0.25 wt-% in Er pins.
- Case 6:** Reference EPR MOX lattice. Three types of MOX pins containing 5.55, 10.4 and 12.0 wt-% plutonium. Uranium enrichment 0.25 wt-%.

The pin layouts of the heterogeneous assemblies are given in Figure 2. For simplicity, the density of the fuel in all pin types (UOX, UOX+BA, MOX) is fixed to 10.5 g/cm<sup>3</sup>.

#### 4.2.2 MOX-UE Cases

The advanced MOX-UE design concept uses additional moderation to compensate for the hardening of the neutron spectrum induced by the plutonium isotopes. The additional moderation is induced using tubular water rods with inner and outer diameter identical to the fuel cladding. The use of 36 water rods lowers the local volumetric fuel-to-moderator ratio from 0.58 to 0.47. The layout of the water rods is shown in Figure 2. It should be noted that this layout differs from that given in reference [2]. The water rods are not as evenly distributed as in the original design, but this improvised layout retains the  $\pi/4$  symmetry of the geometry. The calculation cases are:

- Case 7:** MOX-UE lattice with MOX-A (1st cycle) fuel. Uranium enrichment 0.25 wt-%, plutonium content 9.0 wt-%.
- Case 8:** MOX-UE lattice with MOX-B (equilibrium cycle) fuel. Uranium enrichment 3.0 wt-%, plutonium content 12.0 wt-%.
- Case 9:** MOX-UE lattice with MOX-A fuel including additional americium. Uranium enrichment 0.25 wt-%, plutonium content 9.0 wt-%, americium content 1.0 wt-%.
- Case 10:** MOX-UE lattice with MOX-B fuel including additional americium. Uranium enrichment 3.0 wt-%, plutonium content 12.0 wt-%, americium content 1.0 wt-%.
- Case 11:** MOX-UE lattice with MOX-C (combined 1st and 2nd cycle) fuel including additional americium. Uranium enrichment 2.05 wt-%, plutonium content 12.0 wt-%, americium content 1.0 wt-%.

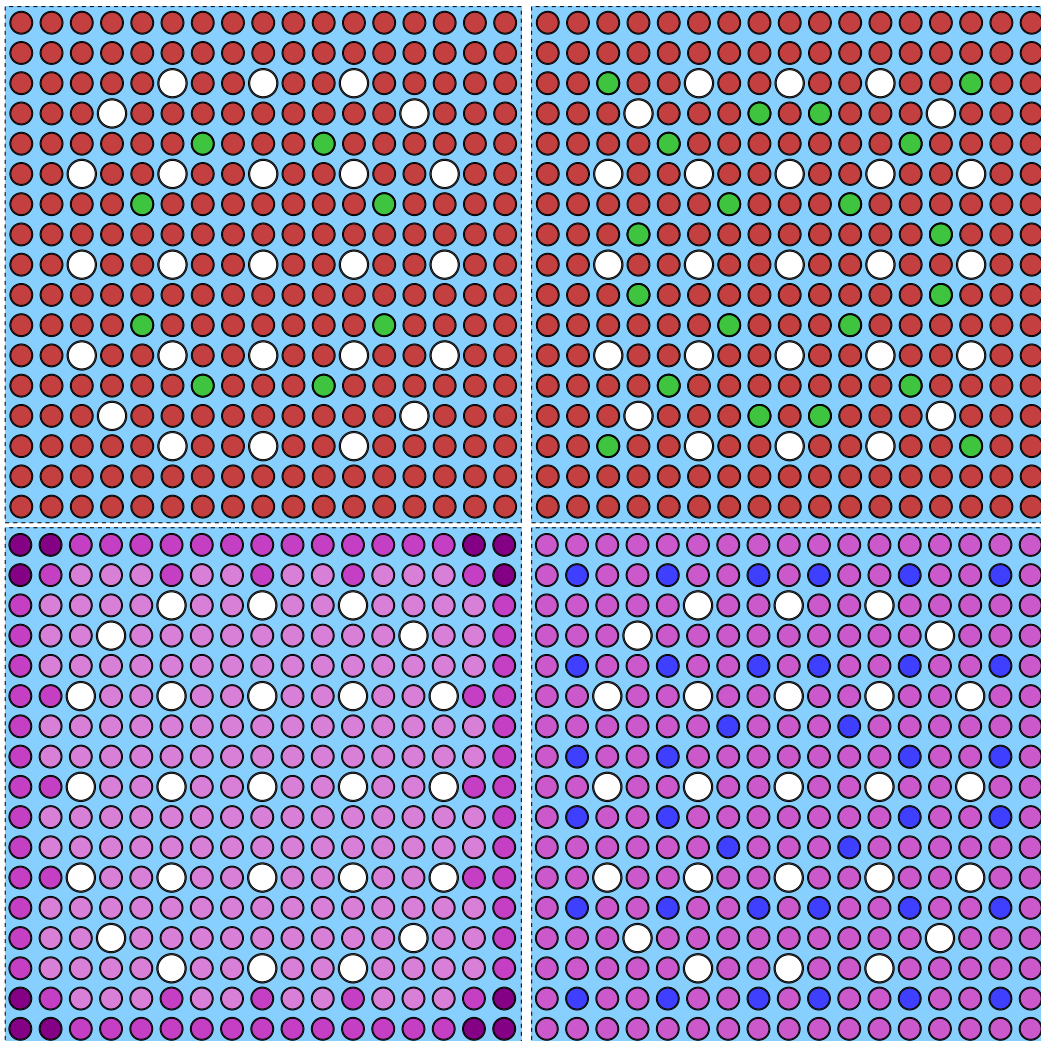


**Figure 2.** Cross-sectional views of the reference EPR UOX assemblies with 8 and 20 burnable absorber pins (green), the heterogeneous EPR MOX assembly with three different plutonium contents (the darkest shade corresponds to the highest concentration) and the homogeneous MOX-UE assembly with additional moderator rods (dark blue).

- Case 12:** MOX-UE lattice with MOX-A fuel including additional americium and curium. Uranium enrichment 0.25 wt-%, plutonium content 9.0 wt-%, americium content 1.0 wt-%, curium content 1.0 wt-%.
- Case 13:** MOX-UE lattice with MOX-B fuel including additional americium and curium. Uranium enrichment 3.0 wt-%, plutonium content 12.0 wt-%, americium content 1.0 wt-%, curium content 1.0 wt-%.

**Case 14:** MOX-UE lattice with MOX-C fuel including additional americium and curium. Uranium enrichment 2.05 wt-%, plutonium content 12.0 wt-%, americium content 1.0 wt-%, curium content 1.0 wt-%.

### 4.3 Calculated Parameters

Various safety-related parameters were calculated using MCNP. The methods used for each parameter are described in the following.

#### 4.3.1 Fuel Temperature Coefficient

Reactivity feedback from fuel temperature results from the Doppler broadening of capture resonance peaks of non-fissile actinides, mainly U-238 and Pu-240<sup>4</sup>. The fuel temperature coefficient is defined as

$$\alpha_{dc} = \frac{d\rho}{dT_f} \approx \frac{\Delta\rho}{\Delta T_f},$$

where  $\Delta\rho$  is the change in reactivity corresponding to  $\Delta T_f$  change in fuel temperature (in K).

Doppler broadening is not included in the calculation procedures of MCNP and the temperature dependence of the nuclear data can only be taken into account by using cross section libraries generated at different temperatures. The nominal fuel temperature in the calculations is 900K. The Doppler coefficient was determined by repeating the calculations using cross section libraries generated at 1200K temperature.

#### 4.3.2 Moderator Temperature Coefficients

Changes in the moderator temperature affect the neutron multiplication in two different ways. First, the moderator density is changed, which directly affects the slowing-down process of fast neutrons. Increasing the moderator temperature decreases the density, which results in the hardening of the neutron spectrum. In this study, this effect is evaluated using the moderator void coefficient:

$$\alpha_{mvc} = \frac{d\rho}{dV_m} \approx \frac{\Delta\rho}{\Delta V_m},$$

where

$$\Delta V_m = \frac{\Delta \varrho_m(T)}{\varrho_m(T)}$$

---

<sup>4</sup>The thermal expansion of the fuel rods also has a noticeable impact in reactivity. This effect, however, is difficult to model properly using a two-dimensional geometry and is therefore omitted.

is the relative change in the moderator density, or in other terms, the absolute change in the moderator void fraction<sup>5</sup>. In practise, the reactivity calculated at full moderator density is compared to the reactivity calculated for moderator density reduced by 10% of the nominal value. At the operational pressure, this reduction in density corresponds to about 24.9 K increase in temperature. For the sake of consistency, the moderator void coefficient is actually expressed using this temperature difference instead of the relative difference in density.

The second moderator feedback effect results from the spectral shift of the Maxwellian peak of thermalised neutrons. This shift is caused by the change in the molecular temperature of hydrogen atoms. The moderator temperature coefficient is defined as:

$$\alpha_{mtc} = \frac{d\rho}{dT_m} \approx \frac{\Delta\rho}{\Delta T_m},$$

where  $\Delta T_m$  is the change in moderator temperature (in K). This change is implemented by replacing the 600K thermal scattering libraries used for the nominal temperature with libraries generated at 800K. The density of the water remains unchanged.

### 4.3.3 Soluble Absorber

The reactivity effect of the soluble absorber is calculated as a differential worth, similar to the reactivity coefficients. Due to this similarity, the boron worth is measured using the moderator boron coefficient, defined as:

$$\alpha_{mbc} = \frac{d\rho}{dC_b} \approx \frac{\Delta\rho}{\Delta C_b},$$

where  $\Delta C_b$  is the change in the moderator boron concentration (in ppm). Concentrations of 0 and 1500 ppm are used for the comparison.

### 4.3.4 Control Rod Worths

The two-dimensional model only allows the calculation of the full control worths of the B<sub>4</sub>C and AIC rods. These worths are calculated by comparing the reactivity of the assembly without control rods to the case in which the rods are fully inserted.

### 4.3.5 Delayed Neutron Fraction

The standard MCNP4C code provides no means to calculate the delayed neutron yields of fission reactions. The delayed neutron data exists, however, in the ACE format cross

---

<sup>5</sup>To be precise, these two definitions are not exactly equivalent, since the “void” in the moderator is actually vaporised water with non-zero density.

section data files, provided that the data is available in the initial evaluation.

The delayed neutron parameters are extracted from the data using a tallyx-subroutine written for the purpose. This subroutine enables an additional multiplier to be used with the standard cell flux tally. This multiplier gives the delayed nuubar times the fission cross section of the corresponding isotope. The effective delayed neutron fraction can then be estimated using:

$$\beta_{\text{eff}} = \frac{\int_E \int_V \phi(E, \mathbf{r}, \hat{\Omega}) \bar{\nu}_d(E) \Sigma_f(E) dE dV}{\int_E \int_V \phi(E, \mathbf{r}, \hat{\Omega}) \bar{\nu}_t(E) \Sigma_f(E) dE dV}. \quad (3)$$

The integral in the denominator can be calculated using the standard cell flux tally with the appropriate multipliers.

It should be noted that the method used here is an approximation from the physical point-of-view in that it estimates the flux-weighted fraction of fission neutrons emitted as delayed. This fraction is not equivalent with the actual definition of  $\beta_{\text{eff}}$ , which essentially means the “importance” of delayed neutrons for the fission rate in the reactor core. According to transport theory, the physically correct method would be to use the adjoint flux as the weighting function. An alternative method, more suitable for Monte Carlo calculations, would be to estimate the fraction of fission reactions induced by delayed neutrons. The topic of calculating  $\beta_{\text{eff}}$  using Monte Carlo techniques is discussed in reference [14]. According to the results presented there, the use of definition (3) is usually a good approximation.

The use of a single fraction for all delayed neutrons without any information on the average emission time gives only a limited description of the kinetic behaviour of the reactor core. A more accurate procedure would be to use group-wise delayed neutron data together with the corresponding average emission times (or the decay constants of the representative precursor groups). It was decided, however, that the simple treatment is sufficient for the purpose of this study.

#### 4.3.6 Prompt Neutron Lifetime

In reactor kinetics, the prompt neutron lifetime,  $l_p$ , is defined as the average time between the emission of a fission neutron and its final absorption in the active part of the reactor core. The prompt neutron lifetime, together with the effective delayed neutron fractions and the corresponding emission times, determines the kinetic behaviour of the chain reaction. The prompt neutron lifetime also defines the dominant time constant in prompt supercritical conditions, i.e. when the reactivity exceeds the effective delayed neutron fraction.

The MCNP4C code does not distinguish between neutrons absorbed in active or inactive parts of the geometry, and hence the accurate calculation of  $l_p$  is not possible.

There are, however, two time constants that can be used for similar purposes. The fission lifespan,  $l_f$ , gives the average time between two fissions in the chain reaction. This parameter hence gives an estimate on how fast a single “reaction chain” propagates. The other useful quantity is the prompt removal lifetime, which gives the average time between the emission of a fission neutron and its final absorption anywhere in the geometry. Since all geometry regions in the two-dimensional model are a part of the active core, this parameter is essentially equivalent with the prompt neutron lifetime, and is therefore denoted by  $l_p$ . It should be noted that the time constants calculated for an infinite lattice are always shorter than the corresponding full-core values, since there is no reflector region in which the neutrons can spend significant time before diffusing back into the fuel.

#### 4.3.7 Local Peaking Factor

Various safety limitations, such as the DNB<sup>6</sup> margin, are determined by the maximum power of the hottest fuel rod in the core. This maximum power is estimated by calculating the radial and axial peaking factors over the entire core using full-core nodal diffusion codes and combining these results to the pin-wise power profile within each node given by more detailed assembly-level calculations. The local power distribution is characterised by the local peaking factor, which is defined as the maximum pin power relative to the assembly average. The pin-wise power distribution can be directly calculated using MCNP and the local peaking factor is calculated for each case.

#### 4.3.8 Performance Indicators

The assessment of fuel performance for burning plutonium and minor actinides is rather difficult in steady state calculations. The main reason for this is that the reaction rates do not remain constant over the irradiation cycle, as the buildup of new isotopes induces various self-shielding effects. This is especially the case for the UOX fuels. Any reaction rate calculations hence apply only to the beginning of cycle conditions with fresh fuel.

Some reaction rates were calculated, however, to get some insight into the buildup rates of actinides. This information may also become valuable when planning the next stage of calculations. The transmutation performance is assessed using the fission-to-capture ratio, which roughly gives the number of destroyed (fissioned) nuclei per nuclei transmuted higher in the actinide chain.

---

<sup>6</sup>Departure from Nucleate Boiling



### 4.3.9 Spectral Quantities

In order to better understand some of the calculated results, the production and absorption spectra are also calculated for each case. The entire energy spectrum ranging from  $10^{-11}$  to 20 MeV is divided into groups with equal lethargy width. Each energy decade is divided into 50 groups, so that the total number of energy groups is 617.

The production spectrum gives the energy distribution of the fission neutron production rate (prompt + delayed). In other words, this distribution shows which energy regions are most important for neutron production. Similarly, the absorption spectrum gives the energy distribution of the neutron absorption rate (capture + fission), or which energy regions are significant for neutron absorption. In addition to the differential spectra, also the integral production and absorption spectra are calculated.

## 5 Results

### 5.1 Production and Absorption Spectra

The results of the spectral calculations are plotted in Figures 3-30. The differential spectra are given as neutrons produced or absorbed per energy unit (MeV). It can be seen that the thermal region is more pronounced for the UOX lattices. The additional low-energy resonances of the plutonium isotopes are clearly seen as peaks and gaps in the MOX fuel spectra. The impact of Pu-240 capture peak at 1 eV is particularly noticeable.

The production or absorption spectrum integrated over the energy range gives the integral spectrum, or the number of neutrons produced or absorbed by one source neutron absorbed below the corresponding energy. From the integral spectra it can be seen that approximately 75% of fission neutrons in the UOX lattice are produced in fissions initiated by neutrons with energy less than 1 eV. For the MOX lattices this fraction is in the order of 60%. The source contribution of fast fission is about 8% for the UOX lattices and about 15% for the MOX lattices.

### 5.2 Safety Parameters

The reactivity coefficients, control worths and kinetic parameters for the various lattices are given in Table 5. It can be seen that the results are consistent with the predictions given in Section 2.2. The additional epithermal resonance peaks of plutonium and minor actinide isotopes improve the fuel Doppler-coefficient. The moderator temperature coefficient is also more negative, as the thermal Maxwell-Boltzmann peak is shifted towards the resonances when the water temperature increases.

Moderator void coefficient remains negative for the MOX fuels and some of the high-moderated MOX-UE assemblies actually give better results, when compared to the reference UOX case. The use of burnable absorbers improves the feedback coefficients of the UOX fuel, but there seems to be no difference between Gd and Er absorbers. It should be noted that the functional dependence of the moderator void coefficient can be quite non-linear, especially with respect to moderator temperature<sup>7</sup>. The results given by these calculations should hence be considered reliable only near the nominal operating temperature.

Control rods and soluble absorber are approximately 30-50% less effective for the MOX fuels when compared to the reference UOX case. The additional moderation of MOX-UE slightly improves the worth of boric acid compared to the reference MOX assembly. The use of burnable absorbers, especially erbium, slightly improve the control worths for the UOX case.

There are clear differences in the kinetic parameters when the UOX and the MOX fuels are compared, but the differences between the different MOX-UE cases are quite small. The effective delayed neutron fraction is 40-50% lower for the plutonium fuels and the neutron lifetimes are significantly shorter due to the increased absorption. The prompt removal lifetime and the fission life span are very typical for lattice-level calculations. The local peaking factor is about 10% higher for the MOX fuels, due to the higher absorption rate.

### 5.3 Fission Probabilities

The fission-to-capture ratios of actinides depend significantly on the hardness of the neutron spectrum. There are differences up to factors of 2 to 10 for the even-N nuclides (U-238, Pu-240, Am-241, etc.). These isotopes can still be categorised as non-fissile in all cases, since the fission-to-capture ratios are far below unity. Altogether, it is very difficult to compare the performance of the different fuel types in static calculations.

## 6 Summary and Conclusions

The recycling of plutonium and minor actinides in commercial LWR fuel cycles has a significant potential in reducing the radiotoxicity of disposed nuclear fuel. The buildup rate of plutonium can be slowed down in conventional “once-through” MOX cycles, which have been a part of the nuclear strategy in various European countries for several years. The full potential of plutonium-recycling, however, is not utilised. The technology required for the stabilisation of the Pu-inventory can become accessible in the near future,

---

<sup>7</sup>The density of water is certainly not a linear function of temperature near the boiling point.



long before Generation IV technology and multi-tier fuel cycles with actinide-burning fast reactors or accelerator-driven systems.

The key element in plutonium management is multi-recycling, which for light water reactors, requires advanced MOX technology. In this study, the feasibility of the innovative homogeneous MOX-UE assembly with enriched-uranium support and additional moderation is compared to conventional PWR UOX and MOX fuels. This report summarises the first phase of the study. Various safety-related parameters are calculated for the different fuel types using the MCNP4C Monte Carlo transport calculation code.

The results show that there are significant differences in fuel and moderator feedback coefficients, control worths and kinetic parameters. The most significant penalty of using MOX fuel is the degradation of the worths of control rods and soluble absorber. Delayed neutron fractions and neutron lifetimes are significantly shorter for the plutonium fuels. The high-moderated MOX-UE assembly performs slightly better than the conventional MOX assembly in some respects, even if additional americium and curium is added in the fuel. The safety features could possibly be improved by slight design modifications and the use of burnable absorbers.

The results of this study are mainly consistent with previous calculations [2]. Control worths are of the same order in magnitude, but some of the moderator void coefficients are far more negative. The void worths of MOX-UE assemblies with americium in reference [2] are close to zero, or even positive if the Am and Pu contents are too high. These discrepancies may simply be due to the differences in the evaluation method, as reactivity is not a linear function of moderator density. Nevertheless, this issue should be further studied before making any conclusions.

It is not possible to estimate the transmutation efficiency of the different fuel types in steady state calculations. The next phase of this study will involve lattice-level burnup calculations using the deterministic CASMO code and the two Monte Carlo burnup calculation codes, Monteburns and MCB. The safety parameters will also be re-evaluated for irradiated fuels, since it can be expected these values will change as the fuel is burnt.

## References

- [1] G. Sengler et al. *EPR core design*, Nucl. Eng. and Design **187** p. 79-119, 1999.
- [2] G. Youinou, et al. *Plutonium and Americium Multirecycling in the European Pressurized Reactor (EPR) Using Slightly Over-Moderated U-235 Enriched MOX Fuel Assemblies*, Global 2003.
- [3] J. F. Briesmeister (editor) *MCNP –A General Monte Carlo N-Particle Transport Code*, LA-13709-M, Los Alamos National Laboratory, 2000.

- [4] W. M. Stacey, *Nuclear Reactor Physics*, John Wiley & Sons, inc., 2001.
- [5] K. Hesketh et al. *Plutonium Management in the Medium Term, a Review on the OECD/NEA Working Party on the Physics of Plutonium Fuels and Innovative Fuel Cycles (WPPR)*, NEA4451, OECD/NEA, 2003.
- [6] D. Warin, *Status of the French Research Programme for Actinides and Fission Products Partitioning and Transmutation*, in proc. 7th Information Exchange Meeting on Actinide and Fission Product Partitioning and Transmutation, Jeju, Republic of Korea, 14-16 October 2002.
- [7] S. Aniel et al. *Plutonium Multirecycling in PWR. The CORAIL Concept*, ICONE-8, 2000.
- [8] G. Youinou et al. *Heterogeneous Assembly for Plutonium Multirecycling in PWRs: The CORAIL Concept*, Global 2001, 2001.
- [9] A. Vasile et al. *Feasibility Studies of the CORAIL Subassembly for Pu Multirecycling in PWRs*, Global 2003, 2003.
- [10] T. A. Aiwo et al. *Assessment of Heterogeneous PWR Assembly for Plutonium and Minor Actinides Recycle*, Global 2003, 2003.
- [11] H. Golfier et al. *Plutonium and Minor Actinides Recycling in PWRs With the New APA Concepts*, Global 2001, 2001.
- [12] *CEA Annual Report 2002*,
- [13] Private communications with J. Wallenius of the Royal Institute of Technology (KTH), Sweden.
- [14] S. C. van der Marck and R. K. Meulekamp, *Calculating the Effective Delayed Neutron Fraction Using Monte Carlo Techniques*, Physor 2004, 2004.

**Table 5.** Reactivity coefficients, control worths and kinetic parameters calculated for the different lattice configurations.

Case	$\alpha_{dc}$ [pcm/K]	$\alpha_{mvc}$ [pcm/K]	$\alpha_{mtc}$ [pcm/K]	$\alpha_{mbc}$ [pcm/ppm]	$B_4C$ [pcm]	AIC [pcm]	$\beta_{eff}$ [pcm]	$l_p$ [ $\mu s$ ]	$l_f$ [ $\mu s$ ]	peak. factor
UOX ref.	-1.5	-45	-0.7	-4.9	-31756	-24336	740	13.3	17.2	1.07
UOX + 8 Gd	-1.7	-49	-1.7	-5.0	-31702	-24170	744	12.5	16.1	1.10
UOX + 20 Gd	-1.9	-53	-3.2	-5.1	-32465	-24486	750	11.4	14.7	1.18
UOX + 8 Er	-1.7	-49	-1.8	-5.1	-32182	-24685	742	13.1	17.0	1.09
UOX + 20 Er	-1.8	-55	-3.5	-5.4	-33367	-25616	745	12.8	16.8	1.17
MOX ref.	-2.3	-44	-1.6	-1.7	-19010	-13024	400	3.6	4.5	1.13
MOX-UE (A)	-2.2	-57	-1.7	-2.8	-22998	-16371	362	5.4	7.1	1.20
MOX-UE (B)	-2.1	-44	-1.5	-2.3	-19522	-13679	447	4.4	5.7	1.20
MOX-UE (A + Am)	-2.3	-66	-2.2	-2.9	-23745	-16892	369	5.0	6.6	1.21
MOX-UE (B + Am)	-2.2	-46	-1.9	-2.3	-19832	-13875	452	4.1	5.3	1.20
MOX-UE (C + Am)	-2.1	-45	-1.9	-2.2	-19393	-13531	426	4.0	5.1	1.20
MOX-UE (A + Am + Cm)	-2.4	-67	-2.1	-2.9	-23773	-16944	367	4.9	6.5	1.21
MOX-UE (B + Am + Cm)	-2.3	-47	-1.9	-2.3	-19812	-13920	449	4.1	5.3	1.20
MOX-UE (C + Am + Cm)	-2.2	-46	-1.9	-2.2	-19398	-13581	423	4.0	5.1	1.20

**Table 6.** Fission-to-capture ratios of actinides calculated for the different lattice configurations.

Case	U-238	Pu-239	Pu-240	Pu-241	Pu-242	Am-241	Am-243	Cm-243	Cm-244	Cm-245
UOX ref.	0.1251	1.7212	0.0027	2.8342	0.0131	0.0109	0.0089	6.3652	0.0606	6.6852
UOX + 8 Gd	0.1270	1.7166	0.0027	2.8296	0.0134	0.0111	0.0090	6.4012	0.0610	6.7067
UOX + 20 Gd	0.1296	1.7101	0.0028	2.8230	0.0140	0.0115	0.0091	6.4540	0.0614	6.7415
UOX + 8 Er	0.1255	1.7225	0.0027	2.8365	0.0131	0.0110	0.0089	6.3623	0.0607	6.6810
UOX + 20 Er	0.1262	1.7243	0.0027	2.8397	0.0132	0.0112	0.0090	6.3587	0.0608	6.6751
MOX ref.	0.1642	1.8126	0.0327	3.1445	0.0539	0.0252	0.0148	6.6043	0.0859	6.8104
MOX-UE (A)	0.1583	1.8253	0.0247	3.0525	0.0369	0.0205	0.0129	6.5908	0.0789	6.7648
MOX-UE (B)	0.1641	1.7986	0.0333	3.0907	0.0799	0.0238	0.0151	6.5645	0.0822	6.7885
MOX-UE (A + Am)	0.1611	1.8223	0.0278	3.0637	0.0389	0.0234	0.0166	6.5527	0.0808	6.7523
MOX-UE (B + Am)	0.1664	1.7978	0.0369	3.1045	0.0830	0.0269	0.0189	6.5247	0.0842	6.7719
MOX-UE (C + Am)	0.1679	1.8114	0.0384	3.1266	0.0594	0.0276	0.0191	6.5570	0.0866	6.7685
MOX-UE (A + Am + Cm)	0.1623	1.8250	0.0281	3.0588	0.0394	0.0237	0.0169	6.5431	0.1301	6.7356
MOX-UE (B + Am + Cm)	0.1676	1.8014	0.0373	3.0984	0.0841	0.0272	0.0193	6.5122	0.1368	6.7508
MOX-UE (C + Am + Cm)	0.1690	1.8150	0.0389	3.1215	0.0601	0.0278	0.0193	6.5468	0.1389	6.7474

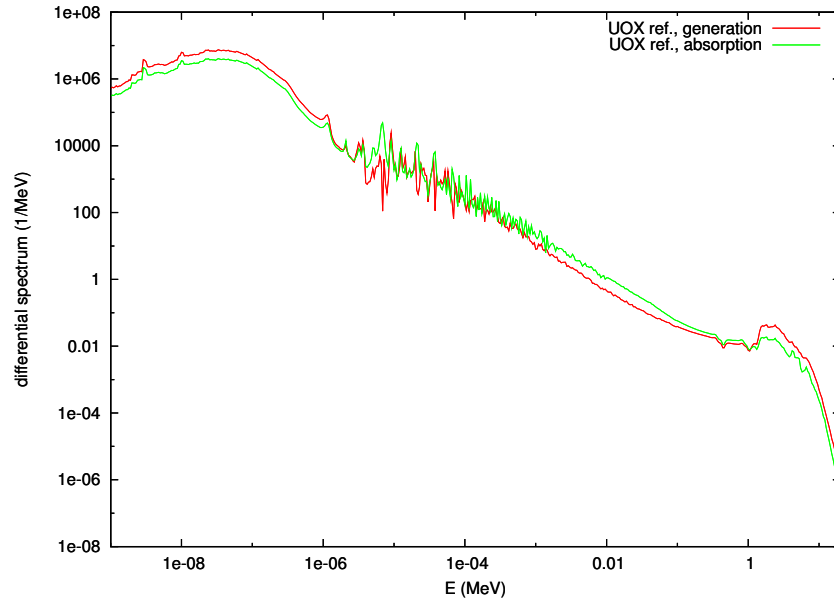


*Figure 3. Differential production and absorption spectra for the UOX reference lattice.*

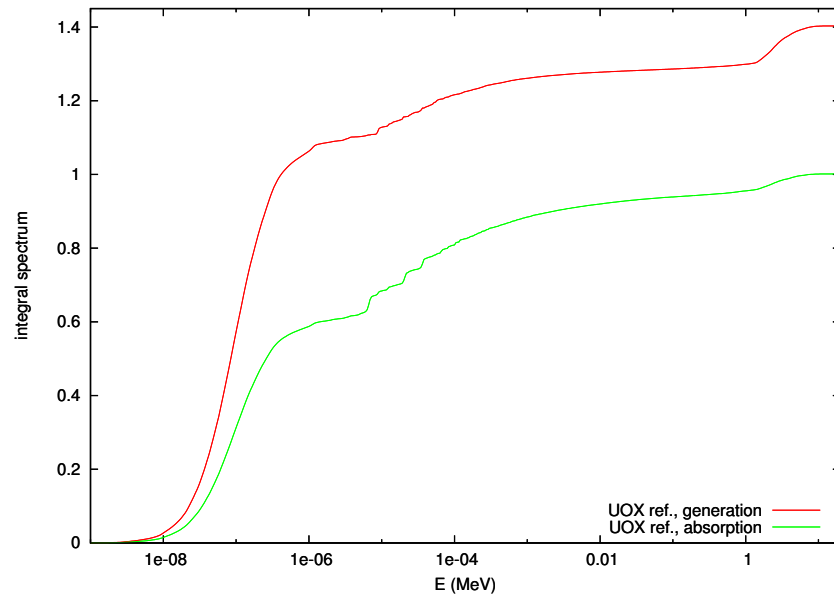


*Figure 4. Integral production and absorption spectra for the UOX reference lattice.*

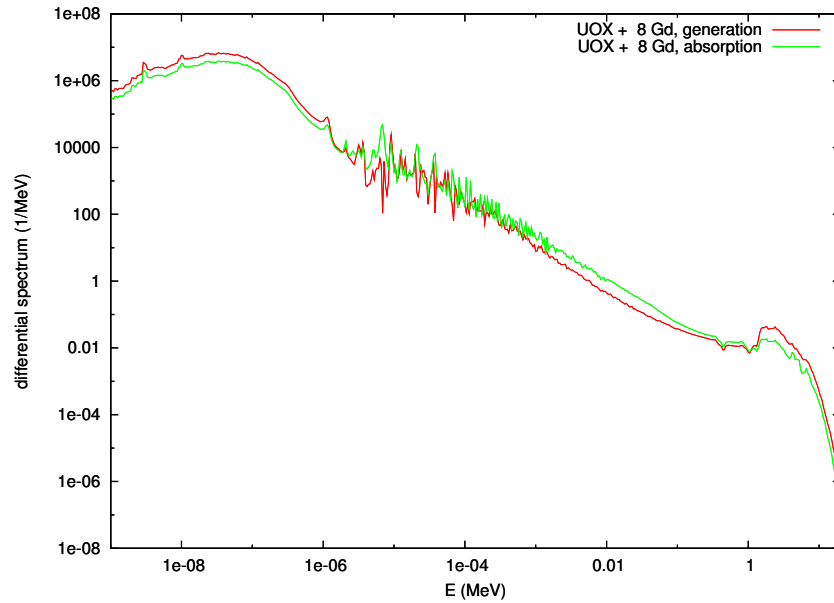


**Figure 5.** *Differential production and absorption spectra for the UOX reference lattice with 8 Gd pins.*

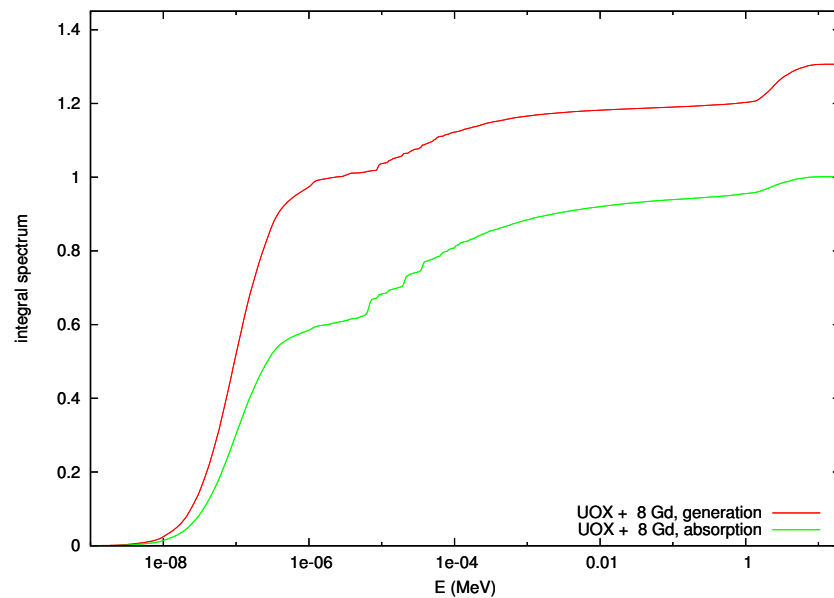


**Figure 6.** *Integral production and absorption spectra for the UOX reference lattice with 8 Gd pins.*

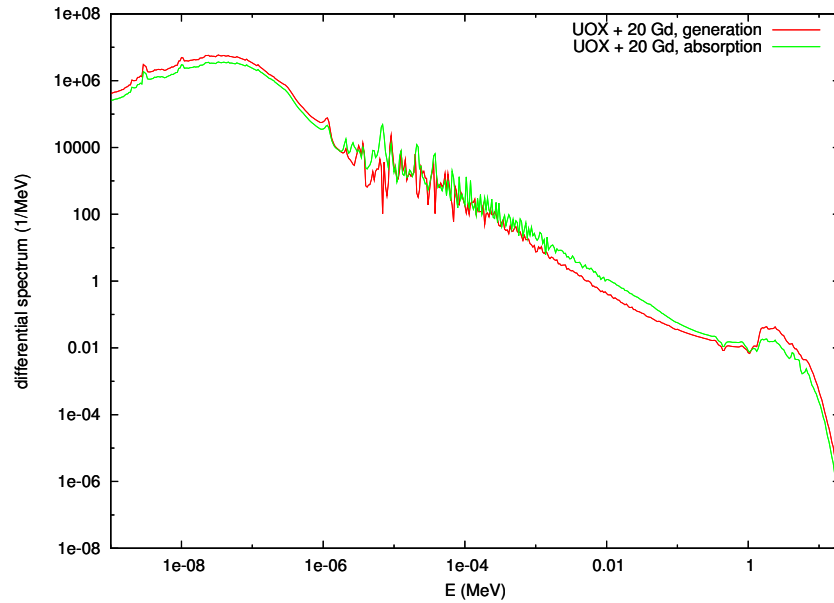


**Figure 7.** *Differential production and absorption spectra for the UOX reference lattice with 20 Gd pins.*

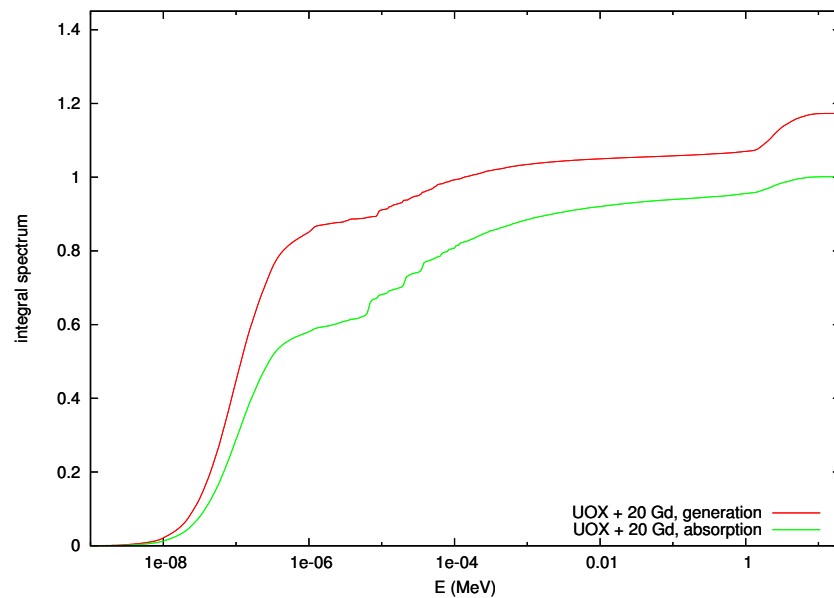


**Figure 8.** *Integral production and absorption spectra for the UOX reference lattice with 20 Gd pins.*

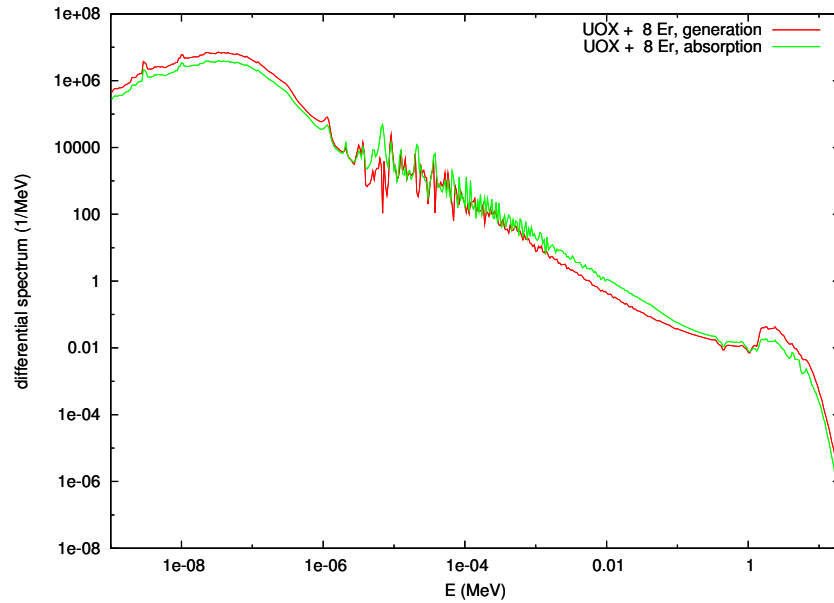


**Figure 9.** *Differential production and absorption spectra for the UOX reference lattice with 8 Er pins.*

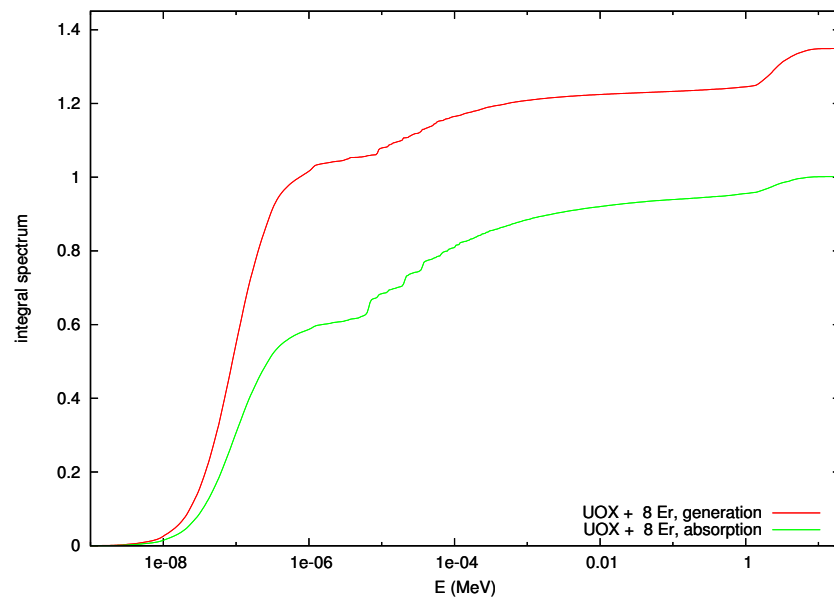


**Figure 10.** *Integral production and absorption spectra for the UOX reference lattice with 8 Er pins.*



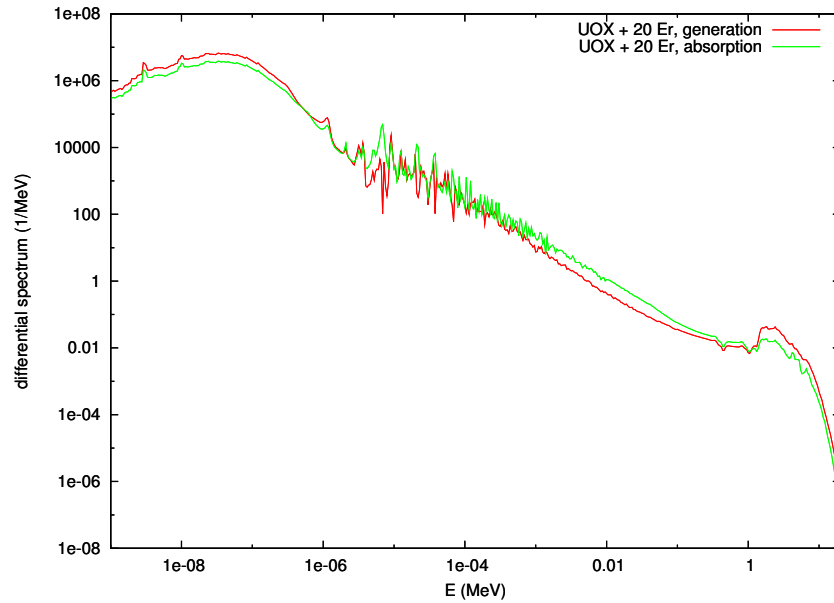


**Figure 11.** *Differential production and absorption spectra for the UOX reference lattice with 20 Er pins.*

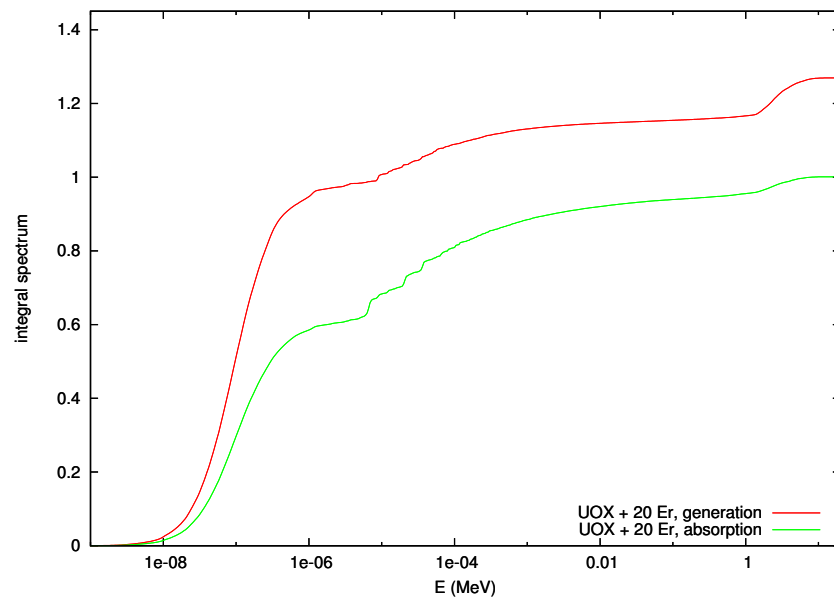


**Figure 12.** *Integral production and absorption spectra for the UOX reference lattice with 20 Er pins.*

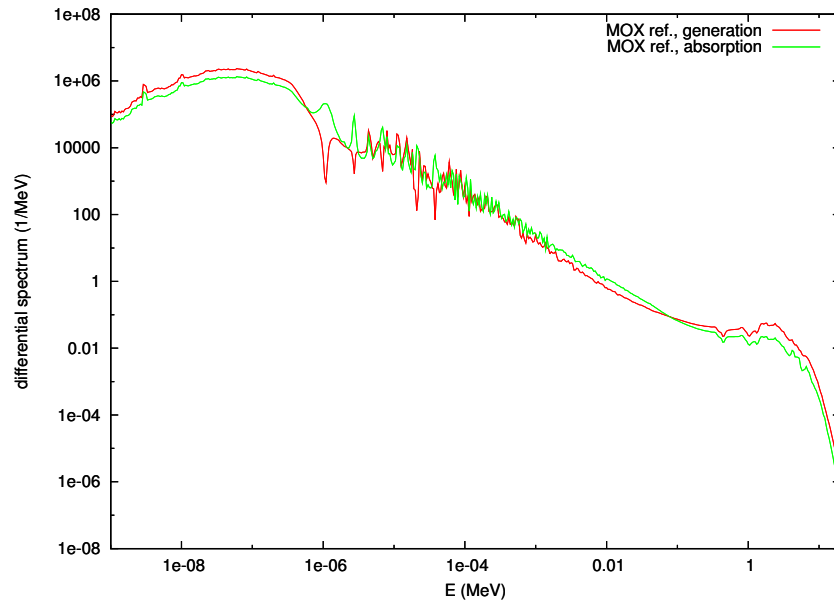


*Figure 13. Differential production and absorption spectra for the MOX reference lattice.*

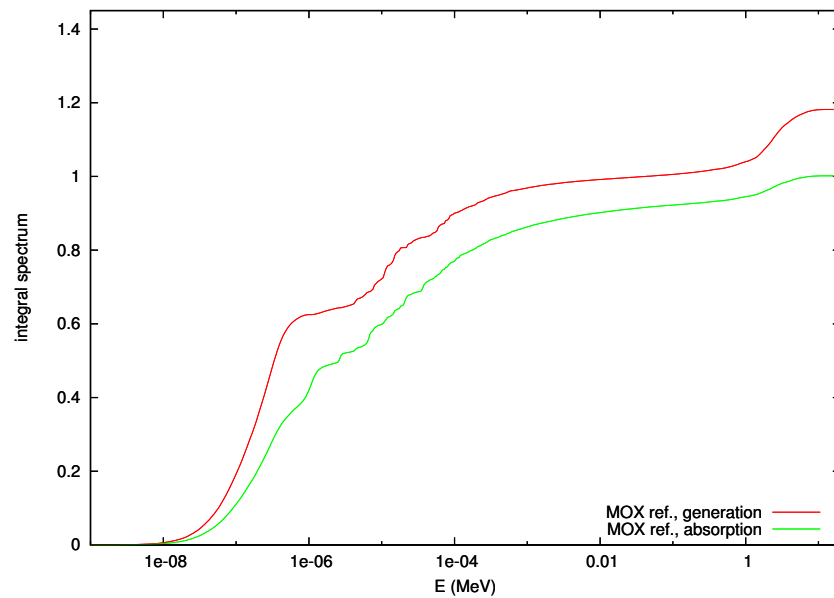


*Figure 14. Integral production and absorption spectra for the MOX reference lattice.*

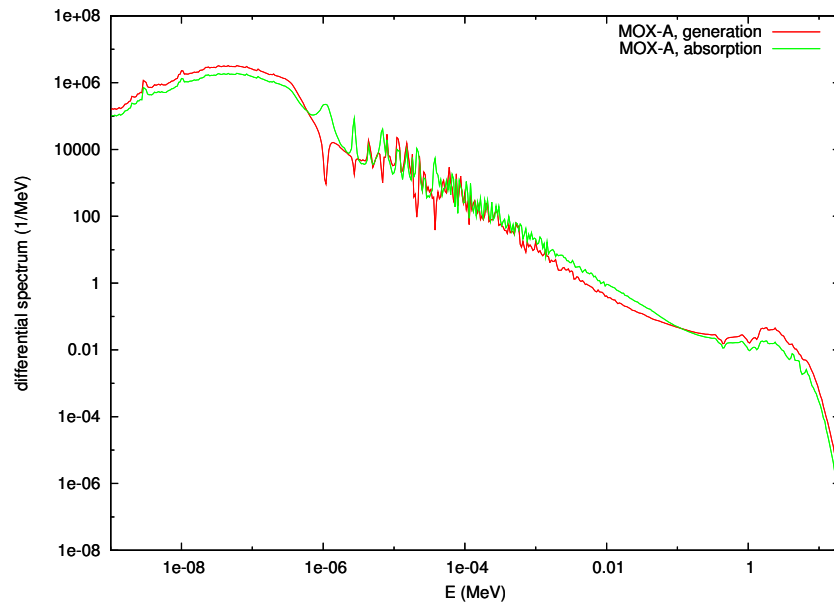


**Figure 15.** *Differential production and absorption spectra for the MOX-UE lattice with MOX-A fuel.*

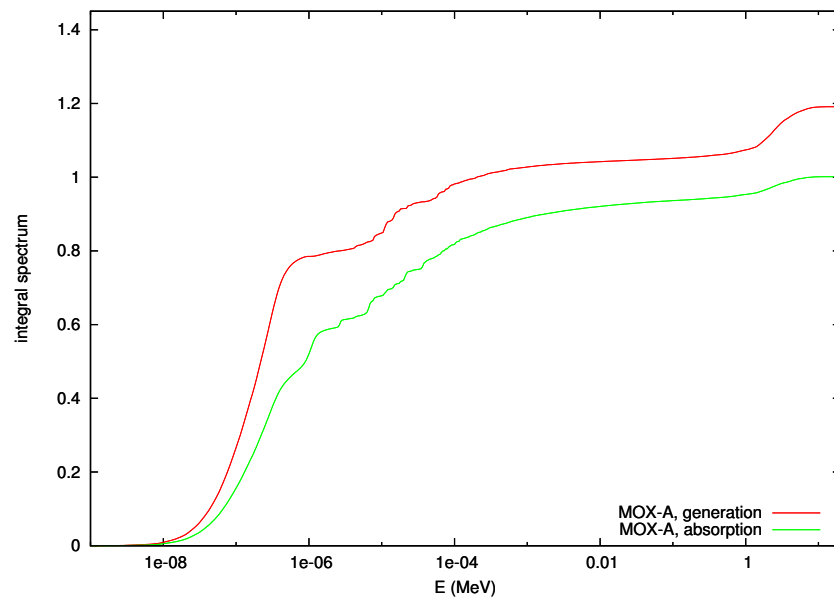


**Figure 16.** *Integral production and absorption spectra for the MOX-UE lattice with MOX-A fuel.*

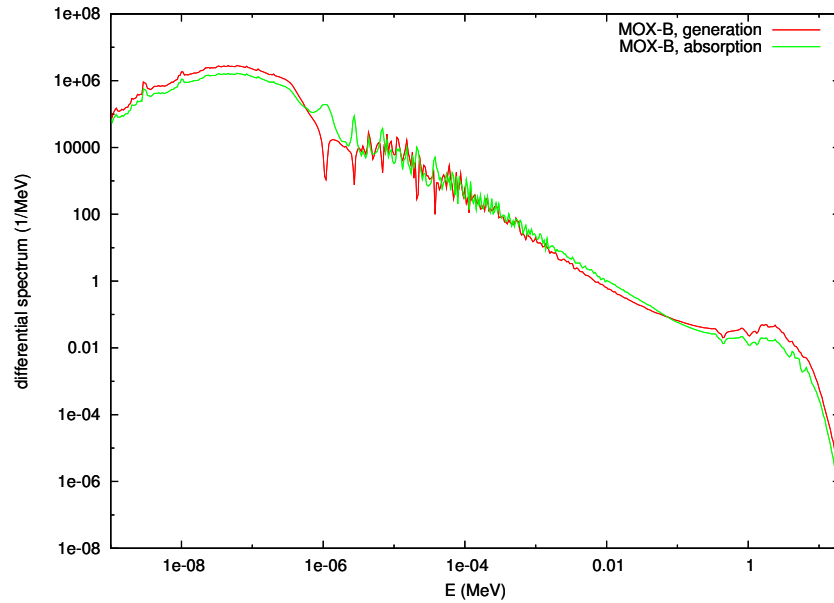


**Figure 17.** *Differential production and absorption spectra for the MOX-UE lattice with MOX-B fuel.*

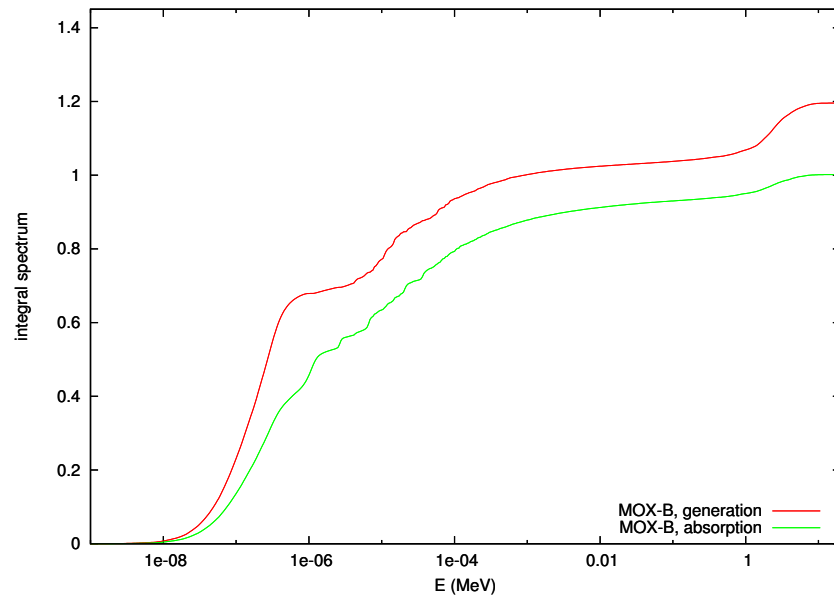


**Figure 18.** *Integral production and absorption spectra for the MOX-UE lattice with MOX-B fuel.*

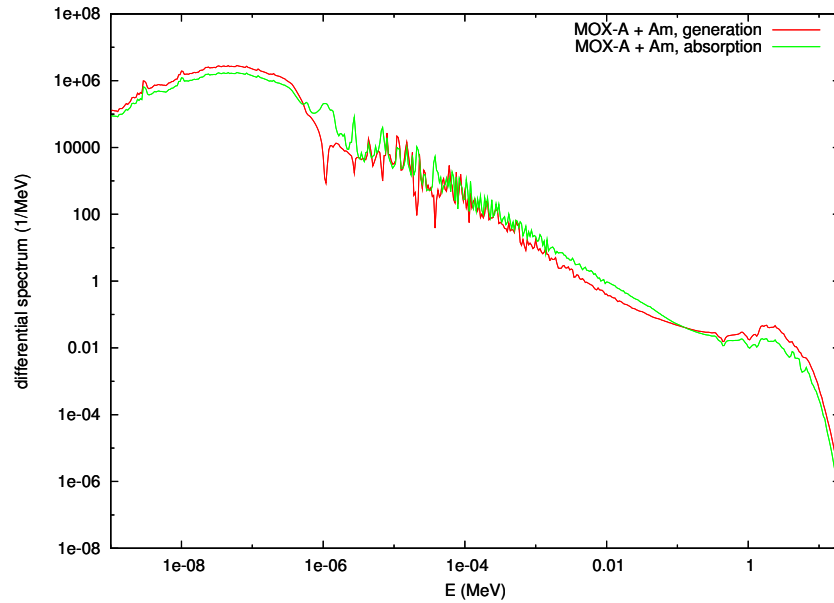


**Figure 19.** Differential production and absorption spectra for the MOX-UE lattice with MOX-A fuel and additional americium.

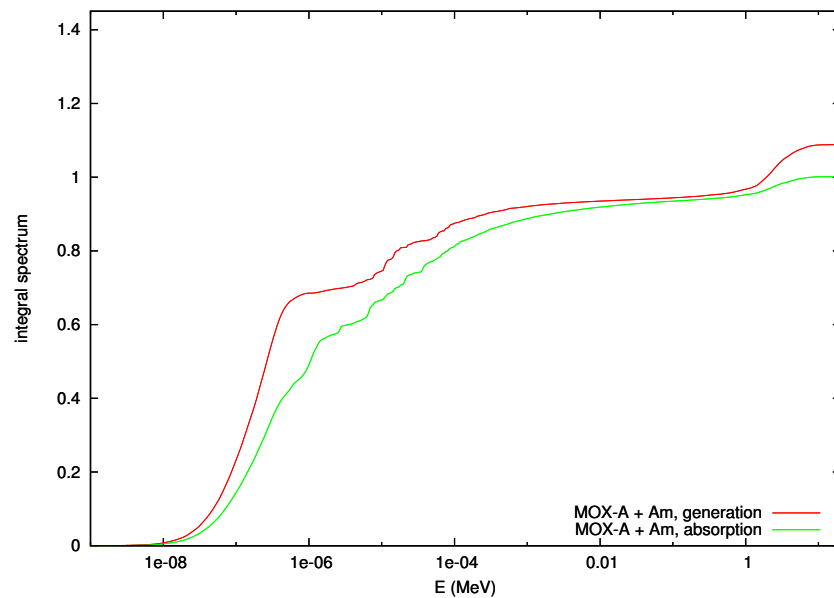


**Figure 20.** Integral production and absorption spectra for the MOX-UE lattice with MOX-A fuel and additional americium.

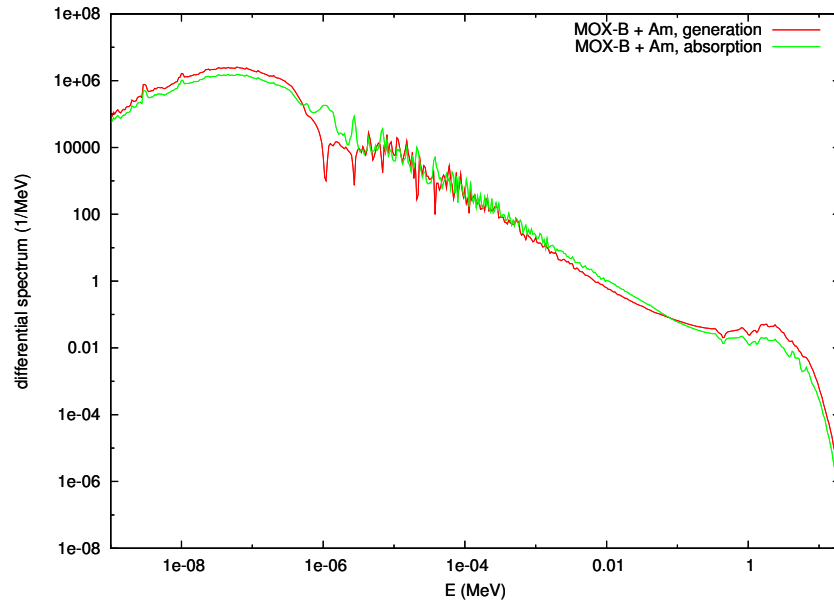


**Figure 21.** Differential production and absorption spectra for the MOX-UE lattice with MOX-B fuel and additional americium.

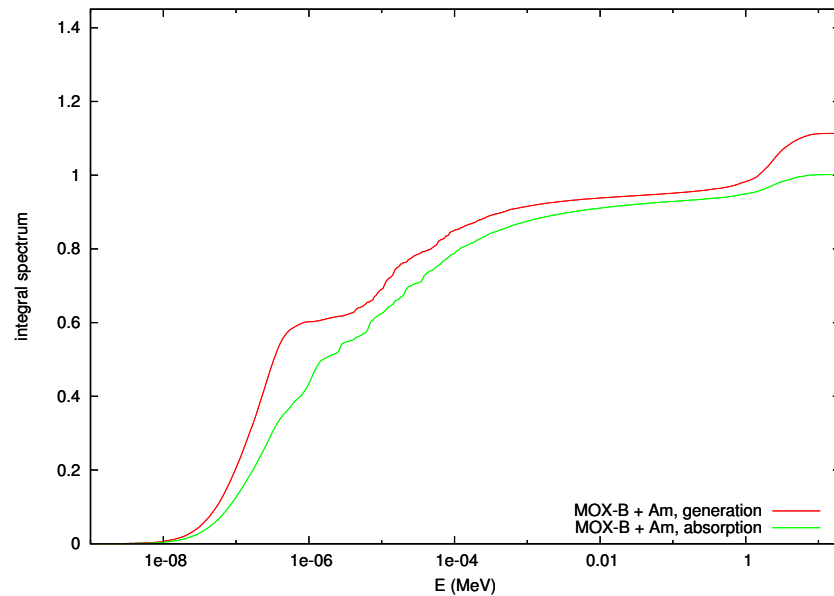


**Figure 22.** Integral production and absorption spectra for the MOX-UE lattice with MOX-B fuel and additional americium.

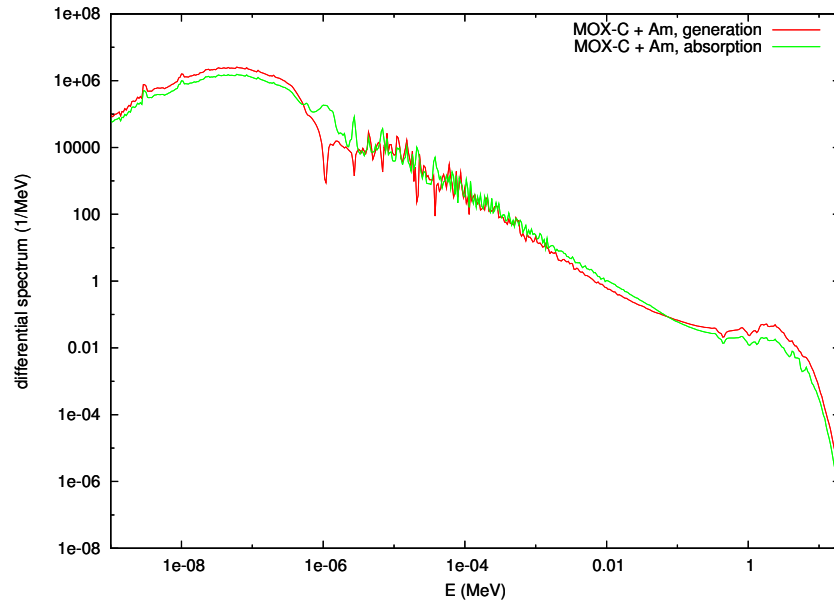


**Figure 23.** Differential production and absorption spectra for the MOX-UE lattice with MOX-C fuel and additional americium.

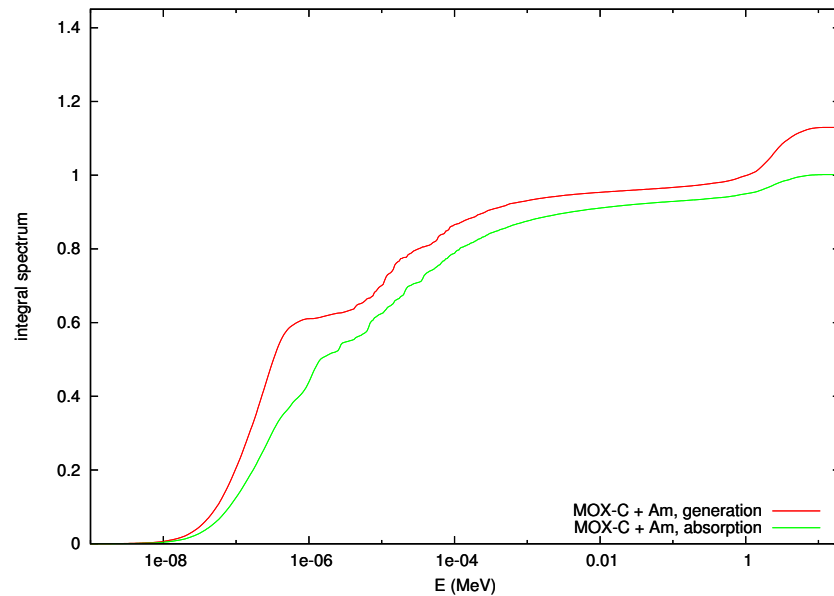


**Figure 24.** Integral production and absorption spectra for the MOX-UE lattice with MOX-C fuel and additional americium.

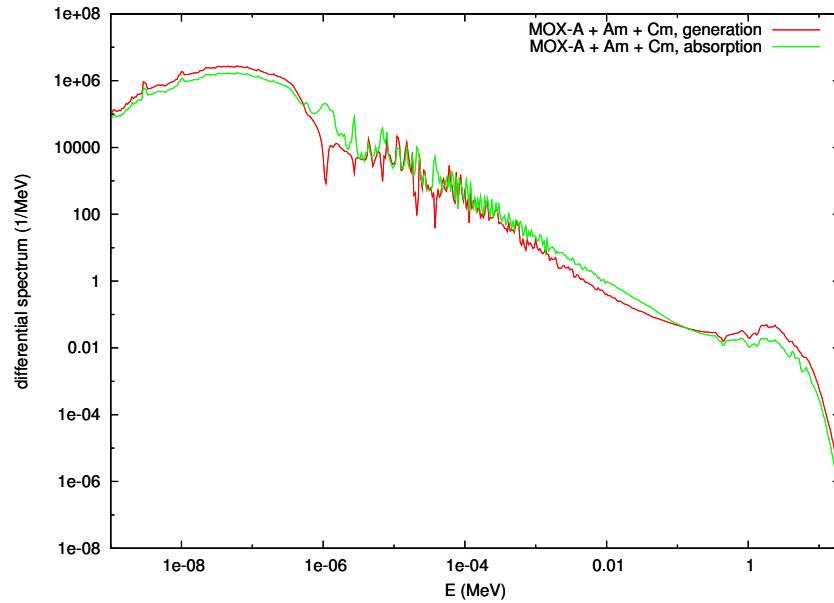


**Figure 25.** *Differential production and absorption spectra for the MOX-UE lattice with MOX-A fuel and additional americium and curium.*

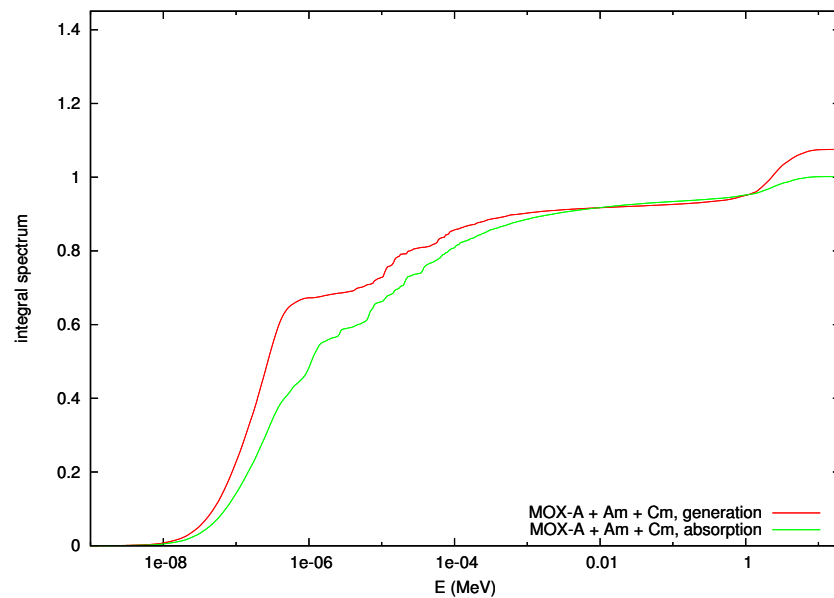


**Figure 26.** *Integral production and absorption spectra for the MOX-UE lattice with MOX-A fuel and additional americium and curium.*



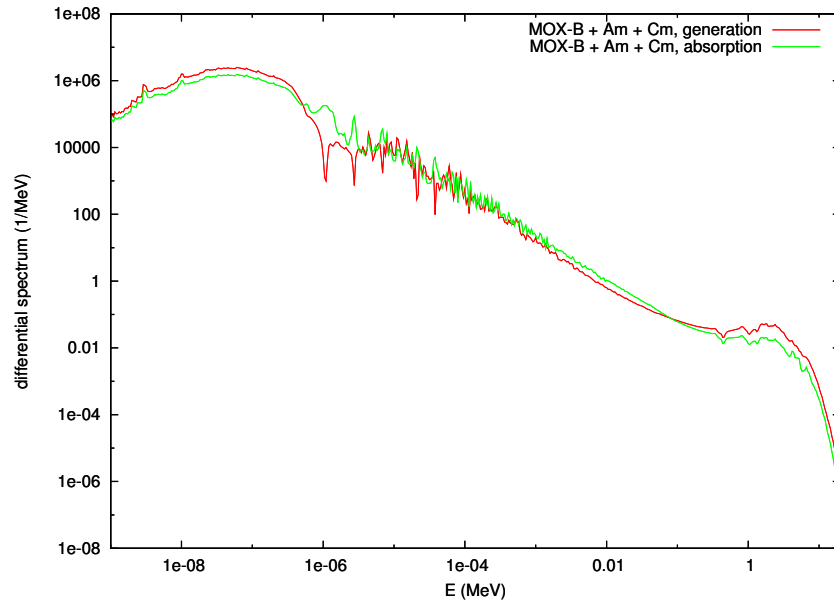


**Figure 27.** Differential production and absorption spectra for the MOX-UE lattice with MOX-B fuel and additional americium and curium.

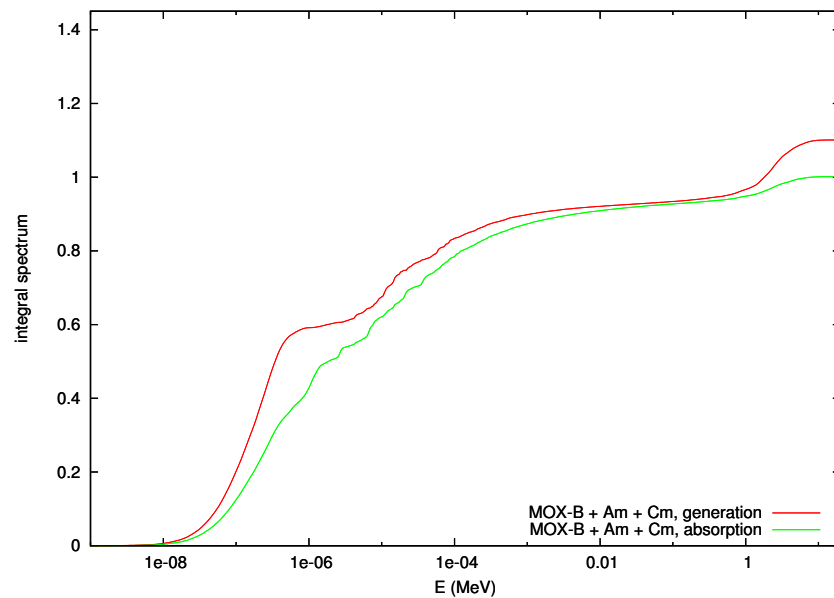


**Figure 28.** Integral production and absorption spectra for the MOX-UE lattice with MOX-B fuel and additional americium and curium.

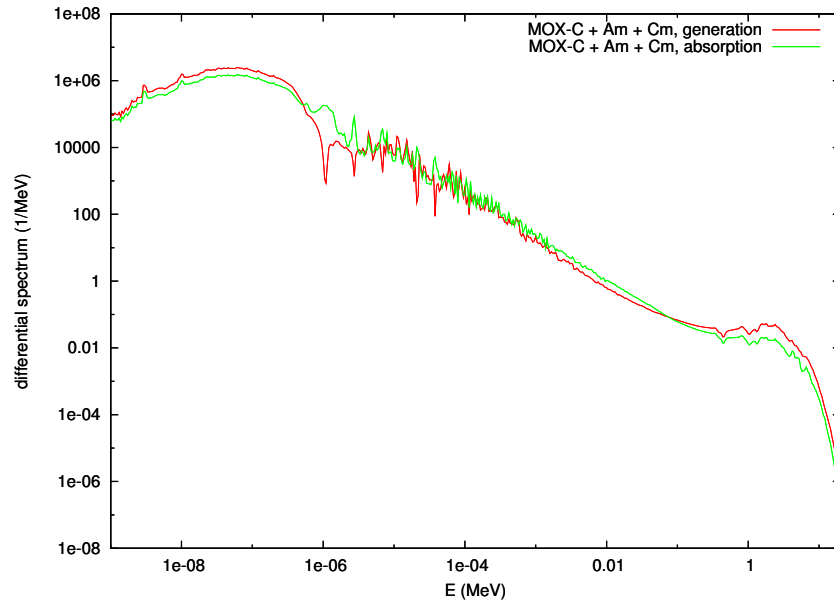


**Figure 29.** Differential production and absorption spectra for the MOX-UE lattice with MOX-C fuel and additional americium and curium.

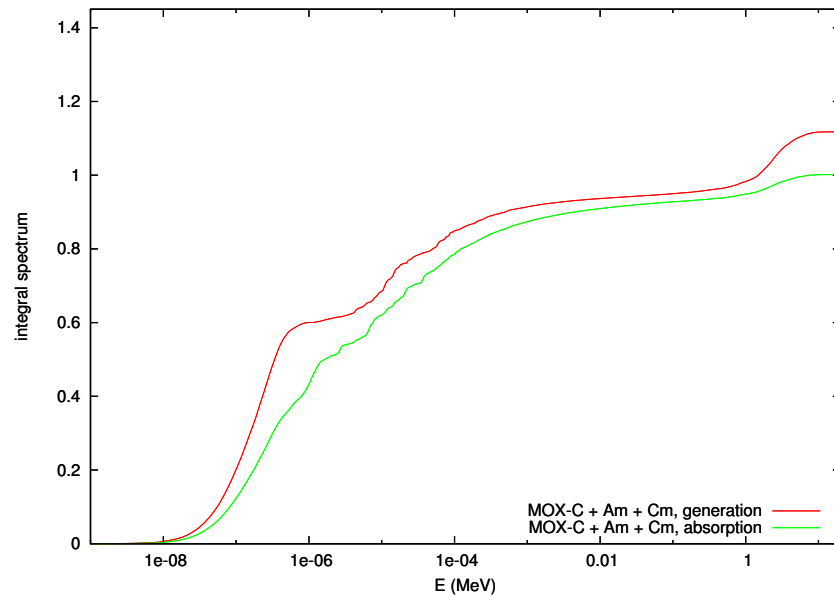


**Figure 30.** Integral production and absorption spectra for the MOX-UE lattice with MOX-C fuel and additional americium and curium.